Journal of Neuroscience Methods 171 (2008) 174–179

Contents lists available at ScienceDirect

Journal of Neuroscience Methods

journal homepage: www.elsevier.com/locate/jneumeth

High throughput quantification of mutant huntingtin aggregates

Emma L. Scotter[a], Pritika Narayan[a,b], Michelle Glass[a], Mike Dragunow[a,b,*]

[a] Department of Pharmacology and Clinical Pharmacology, Faculty of Medical and Health Sciences, The University of Auckland, Auckland, New Zealand
[b] National Research Centre for Growth and Development, The University of Auckland, Auckland, New Zealand

ARTICLE INFO

Article history:
Received 19 December 2007
Received in revised form 12 February 2008
Accepted 12 February 2008

Keywords:
Huntington's
Aggregate
Discovery-1

ABSTRACT

Mutant protein aggregates are an important biomarker in Huntington's and other neurodegenerative diseases however their quantification has typically relied on manual imaging and counting, or cell-free assays, which do not allow for concurrent analysis of cell viability. Here we describe four automated high throughput image analysis methods, developed using Metamorph™ software, to quantify mutant huntingtin aggregates in a cellular context. Imaging of aggregate-forming cells was also automated, using a Discovery-1™ automated fluorescence microscope. All four analysis methods measured aggregate formation accurately in relation to manual counting, but with differing throughput. Our in-house PolyQ assay gave the highest throughput, processing images at 0.31 s per image. The Cell Scoring assay gave lower throughput, at 19.5 s per image, but offered accurate quantification of the proportion of cells which formed aggregates, without bias from cell death. These image analysis tools provide rapid and objective alternatives to manual counting in studies of aggregate formation, to facilitate the discovery of drugs to treat Huntington's and related neurodegenerative diseases.

1. Introduction

Huntington's disease (HD) is a heritable neurodegenerative disorder characterised by striatal and cortical cell loss. Expansion of a polyglutamine stretch within the huntingtin protein leads to the formation of protein aggregates in the areas of cell loss (The Huntington's Disease Collaborative Research Group, 1993). Whether huntingtin protein aggregates are a cause or result of cellular degeneration is a controversial issue. Support for a cytotoxic role for huntingtin protein aggregates comes from studies which show molecular (Heiser et al., 2002; Muchowski et al., 2000; Sanchez et al., 2003) and/ or behavioural (Sanchez et al., 2003) 'rescue' through the prevention of protein aggregation. Conversely, several studies suggest that aggregation is a cellular survival mechanism designed to sequester mutant protein from interacting aberrantly with other proteins (Arrasate et al., 2004; Saudou et al., 1998).

In either case, quantification of these protein aggregates is used to evaluate the effect of drug therapies in HD, yet a high throughput image-based analysis of aggregate formation has yet to be described. Current methods depend upon either low throughput manual counting of aggregates (Corcoran et al., 2004; Kitamura et al., 2006; Skogen et al., 2006), or cell-free aggregate elongation/ dye incorporation assays which do not allow for concurrent analysis of cell health or, therefore, the applied therapeutic potential of drugs (Berthelier and Wetzel, 2006; Hamuro et al., 2007; Kato et al., 2007).

The use of indirect measures of aggregate formation, such as fluorescent dye incorporation, cannot delineate between changes in aggregate number and changes in aggregate size/density. If the sequestration of mutant huntingtin into aggregates is indeed a mechanism by which cells target mutant huntingtin for destruction (Ravikumar et al., 2004), drugs which favour many smaller aggregates might be preferable to those which produce fewer large aggregates. Not only are many small aggregates more efficient at recruiting and sequestering soluble mutant huntingtin monomers (Chen et al., 2001), they might potentially allow for more efficient autophagic or proteasomal destruction.

Here we describe a number of high throughput image analysis assays that we have developed for quantifying aggregates of mutant huntingtin. Each of the methods presented here offer a rapid and powerful approach to the screening of drugs, siRNA, or other therapeutics which might alter mutant huntingtin aggregation.

2. Materials and methods

2.1. Culture and maintenance of PC12 N 67Htt cell lines

For this study, stable PC12 cell clones which express N-terminal huntingtin protein following induction with the insect steroid hor-

* Corresponding author at: Department of Pharmacology, Faculty of Medical and Health Sciences, The University of Auckland, Park Road, Grafton, Auckland, New Zealand. Tel.: +649 373 7599x86403; fax: +649 373 7556.
E-mail address: m.dragunow@auckland.ac.nz (M. Dragunow).

0165-0270/$ – see front matter © 2008 Elsevier B.V. All rights reserved.
doi:10.1016/j.jneumeth.2008.02.007

mone tebufenozide were utilised (Aiken et al., 2004; Suhr et al., 1998). The huntingtin constructs comprised the first 67 amino acids with a polyglutamine tract of 25 (non-aggregate forming) or 97 (aggregate-forming) repeats and a C-terminal EGFP tag (N67Htt25Q/97Q) (Kazantsev et al., 1999). PC12 cells were cultured in Dulbecco's modified Eagle's medium (DMEM, Invitrogen, Carlsbad, CA) containing high glucose (4500 mg/l), L-glutamine (4 mM), and sodium pyruvate (110 mg/l) and supplemented with 10% horse serum, 5% fetal bovine serum, 100 units/ml penicillin, 100 μg/ml streptomycin, 25 mM HEPES, and 250 μg/ml geneticin to maintain stable plasmid integration. Cells were grown at 37 °C in a humidified 95% air, 5% CO_2 environment.

2.2. Discovery-1™ image acquisition

Fluorescent images of huntingtin-EGFP expressing cells for both preliminary induction condition studies and for high throughput assay validation studies were acquired at 10× magnification from 4 sites/well using the FITC filter set (470Ex/535Em) and an exposure time of 1000 ms (nearing saturation of the pixel gray values for large huntingtin aggregates but also ensuring detection of small aggregates) on a Discovery-1™ (Molecular Devices, Sunnyvale, CA) automated fluorescence microscope. Corresponding fluorescent images of Hoechst-stained cell nuclei in the same sites were acquired using a DAPI filter set (403Ex/465Em) and an exposure time of 1000 ms. The number of cells per image ranged from 83 to 731 cells.

2.3. Determining conditions for the induction of aggregate formation

Conditions for the induction of aggregates in PC12 N67Htt97Q cells were tested first using a range of tebufenozide concentrations from 0 to 1 μM with an incubation time of 72 h. PC12 N67Htt97Q cells were seeded at 20,000 cells/well, 100 μl/well, 4-well per time point, in poly-L-lysine coated 96-well plates. Cells were induced to express mutant huntingtin the following day by replacement with fresh media (100 μl/well) containing a final concentration of 0–1 μM tebufenozide (Dow Agrosciences, Indianapolis, IN), and were fixed in 4% paraformaldehyde after 72 h. Following 3× washes in phosphate buffered saline (PBS, 0.15 M, pH 7.4), cell nuclei were stained with Hoechst 33258 (Sigma, St. Louis, MO) for 10 min. Cells were finally washed a further 3× in PBS, imaged on a Discovery-1™ automated fluorescence microscope, and aggregate-positive and aggregate-negative cells counted manually from image overlays of the FITC and DAPI channel for each site (image overlays were developed using the 'Colour Combine' function within Metamorph™ analysis software (Molecular Devices)). Data shown represents counts from one site from each replicate well ($n = 3$) from one representative experiment ($n = 3$).

2.4. Confirmation of visually punctate species as aggregates

In order to be sure that the bright fluorescent puncta counted in PC12 N67Htt97Q cells were indeed aggregates, defined by Kazantsev et al. (1999) as 'insoluble detergent-resistant' species, a filter retardation assay was performed. PC12 N67Htt25Q and PC12 N67Htt97Q cells were plated in 6-well plates at 5×10^6 cells/well, 2 ml/well, 5-well per cell type. The following day, cells were induced to express huntingtin-EGFP by replacement of media with fresh media (2 ml/well) containing 1 μM tebufenozide and incubated for 48 h. Cells from all five wells were pooled after harvesting with trypsin. Pooled samples were spun at 1900 × *g* for 5 min, washed in PBS and respun. The resulting pellet was resuspended in 1 ml lysis buffer (50 mM Tris pH 8.8, 100 mM NaCl, 5 mM MgCl, 0.5% NP40, 1 mM EDTA, 1× complete protease inhibitors (Roche, Basel, Switzerland)), incubated on ice for 30 min, and spun at 20,000 × *g* for 5 min. The pellet was resuspended in 300 μl 20 mM Tris pH 8, 15 mM MgCl containing 1 mg/ml DNase1 (Roche), and incubated at 37 °C for 1 h. Protein concentration was determined using the BioRad DC protein assay (BioRad Laboratories, Hercules, CA), and solubilisation buffer was added to give a final concentration of 300 μg/ml protein, 20 mM EDTA, 0.05 M DTT and 10% SDS. Samples were heated at 65 °C for 5 min and 100 μl (30 μg) loaded in triplicate onto a 0.22 μM cellulose acetate membrane (GE Osmonics Inc., Minnetonka, MN) under vacuum using an Easy-Titer© ELIFA system (Pierce, Rockford, IL). Filters were rinsed briefly in 0.2% SDS before fixation in 0.5% gluteraldehyde for 20 min, then washed 3× in TBS-T (10 mM Tris Base, 150 mM NaCl, 0.05% Tween 20).

Filters were then probed for EGFP-tagged, insoluble species retained by the membrane (i.e. huntingtin-EGFP aggregates). Filters were blocked for 30 min in TBS-T containing 1% bovine serum albumin (BSA). α-GFP antibody raised in rabbit (Abcam, Cambridge, UK) was then applied in TBS-T with 0.2% BSA overnight at 4 °C shaking. Filters were washed in TBS-T 3× 10 min and horse radish peroxidase conjugated α-Rabbit IgG antibody (Chemicon, Temecula, CA) applied in TBS-T with 0.2% BSA for 2 h at room temperature shaking. Filters were again washed in TBS-T 3× 10 min and then incubated with ECL plus chemiluminescent reagent (Amersham, Buckinghamshire, UK) for 5 min. Protein dots were detected by exposure to ECL Hyperfilm (Amersham) for 1 h.

2.5. Comparison of high throughput assays for the quantification of mutant huntingtin aggregates

Following validation of the protein concentration- and time-dependent formation of mutant huntingtin aggregates in this model, comparison and evaluation of high throughput assays of aggregate formation was performed on PC12 N67Htt25Q and PC12 N67Htt97Q cells induced over a 120 h time course. Cells were seeded at 20,000 cells/well, 100 μl/well, 4-well per time point, in a separate poly-L-lysine coated 96-well plate for each time point. Cells in all plates were induced to express mutant huntingtin the following day by replacement with fresh media containing 1 μM tebufenozide final, and were fixed in 4% paraformaldehyde at appropriate time points. Following 3× washes in PBS, cell nuclei were stained with Hoechst 33258 for 10 min. Cells were finally washed a further 3× in PBS, imaged on a Discovery-1™ automated fluorescence microscope and analysed using MetaMorph™ image analysis software.

For this study three analysis modules within Metamorph™ and one developed in-house using a combination of Metamorph™ tools were evaluated for their suitability for quantifying huntingtin aggregate formation: Find Spots, Granularity, Cell Scoring and PolyQ (in-house assay). PC12 N67Htt25Q cells express normal huntingtin-EGFP which does not form protein aggregates, whereas the mutant huntingtin-EGFP in PC12 N67Htt97Q cells forms large aggregates. The analysis parameters described for each module were optimised to maintain a balance between maximal detection of small aggregates seen in PC12 N67Htt97Q cells and minimal detection of bright 'puncta' of soluble non-aggregated huntingtin-EGFP in PC12 N67Htt25Q cells.

2.5.1. PolyQ assay

The PolyQ assay used a threshold gray-level range to segment objects in each image which were then counted using an object standard area measure which defines the average size of the object of interest. The object standard allows the counting of clustered aggregates in complexes of cells by determining the number of times larger the total area of the cluster is than the value defined as the standard area of a single aggregate. For this study, a threshold

gray-level range from 585 to 4095 and an object standard of 45 μm^2 was applied.

2.5.2. Find Spots assay

The Find Spots assay segments circular areas of positive staining in individual wavelength channels using intensity (spot cut-off) and size (region size) thresholds. Huntingtin-EGFP aggregates were detected with a spot cut-off of 60 and a threshold region size of 9 (both arbitrary units). Aggregate numbers as assessed by PolyQ and Find Spots commands were normalized to Hoechst-positive cell numbers counted using the Count Nuclei application with the parameters for nuclei being 6–8 μm width range and an intensity of six gray-levels above local background.

2.5.3. Granularity assay

The Granularity assay segments objects in two wavelengths simultaneously, such that nuclei and aggregate counts are performed in a single analysis. The parameters for nuclei counts were 6–8 μm for the width range and an intensity of six gray-levels above local background to match the nuclei count settings used within the Count Nuclei and Cell Scoring applications. In the FITC channel, both cytoplasmic and nuclear huntingtin-EGFP within a 5–10 μm width range and an intensity of 150 gray-levels above local background were counted.

2.5.4. Cell Scoring assay

Like Granularity, the Cell Scoring application module also segments objects in two wavelengths simultaneously. However in this application only Hoechst-positive cells are analysed for huntingtin-EGFP labelling, such that aggregates which are independent of a cell are disregarded. This occurs as a result of the death of the cell which generated the aggregate, and not due to exocytosis or evacuation of the aggregate from a living cell (unpublished observation). For detection of aggregate positive cells, Hoechst-stained nuclei within a 6–8 μm width range and an intensity of six gray-levels above local background were counted. Then both cytoplasmic and nuclear huntingtin-EGFP within a 5–10 μm width range from the margin of a Hoechst-positive nucleus and an intensity of 150 gray-levels above local background were counted.

Results for all assays were logged automatically to Microsoft Excel spreadsheets and analyzed using GraphPad Prism 4 (GraphPad Software Inc., San Diego, CA). To validate the results obtained with the image analysis assays, manual 'blinded' counts were performed on the 48 h data set, and Pearson's correlations and ANOVAs were performed to compare these manual counts with the automated assays.

All experiments and analyses were performed as three independent repeats. Exposure times and therefore analysis parameters were optimised independently for each repeat to ensure image fluorescence was always within the linear range of camera detection given any variance in microplate optics and ambient lighting. Exposure times, analysis parameters and graphs shown are for one representative experiment.

3. Results and discussion

3.1. Puncta of EGFP fluorescence in PC12N67Htt cells are aggregates, whose formation is both concentration- and time-dependent

The tebufenozide-inducible expression system was developed by Suhr et al. (1998) and characterised as a model for HD drug screening in PC12 cells by Aiken et al. (2004). Increasing concentrations of the steroid hormone inducer tebufenozide increase the number of cells containing aggregates of mutant huntingtin-EGFP (Fig. 1). Longer induction times at a fixed inducer concentration also increase the proportion of aggregate-containing cells (Fig. 3). These findings are in agreement with previous reports that huntingtin aggregate formation is both protein concentration- and time-dependent (Scherzinger et al., 1999).

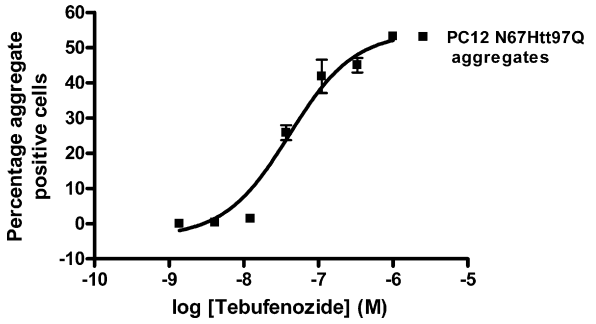

Fig. 1. Manual cell counts of the percentage of PC12 N67Htt97Q cells containing aggregates following induction of mutant huntingtin expression with 0–1 μM tebufenozide for 72 h. The formation of mutant huntingtin aggregates shows a clear dependence upon the concentration of the inducer, tebufenozide, as determined by a one-way ANOVA ($F = 259.7$, $P < 0.0001$). Post hoc Newman–Keuls Multiple Comparison Tests showed that concentrations of tebufenozide at and above 37 nM elicited significant aggregate expression.

The filter retardation assay (Fig. 2) supports the assumption that the discreet puncta of bright EGFP fluorescence formed selectively in PC12N67Htt97Q and not PC12N67Htt25Q cells are indeed 'aggregates'. EGFP-immunoreactivity was found in the SDS-insoluble fraction for induced PC12N67Htt97Q but not PC12N67Htt25Q cells, suggesting that mutant huntingtin forms detergent-resistant aggregates which remain trapped by the cellulose acetate filter, while normal huntingtin is detergent-soluble and passes through the filter.

3.2. Existing and in-house developed Metamorph™ assays offer high throughput aggregate quantification

The automated image analysis assays were far more rapid than the counts performed manually. Manual counts of images of aggregates alone took approximately 56 s per image (this excludes the time required for logging data into Microsoft Excel spreadsheets). The automated counting and logging of results for aggregates alone with the PolyQ assay took 0.31 s per image, Find Spots required 1.25 s per image, and Granularity required 6.25 s per image. The Count Nuclei module, or the equivalent nuclei count within the Granularity assay, required 10 s per image.

All four image analysis methods detected and counted aggregates accurately and in good agreement with the manual counts.

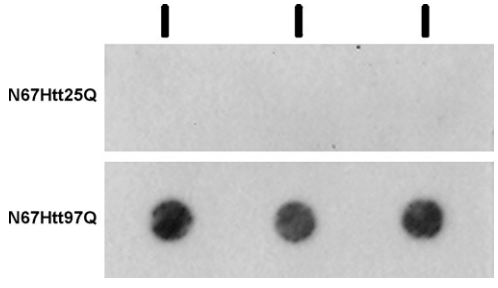

Fig. 2. Filter-trapped, SDS-insoluble, EGFP-positive species in PC12 N67Htt25Q and PC12 N67Htt97Q cells induced to express mutant huntingtin with 1 μM tebufenozide for 48 h. Thirty micrograms insoluble protein was loaded for both PC12 N67Htt25Q and PC12 N67Htt97Q cells (load positions marked by vertical black lines), and mutant (PC12 N67Htt97Q) but not normal (PC12 N67Htt25Q) huntingtin-EGFP was found in this insoluble fraction, confirming that it does indeed form aggregates.

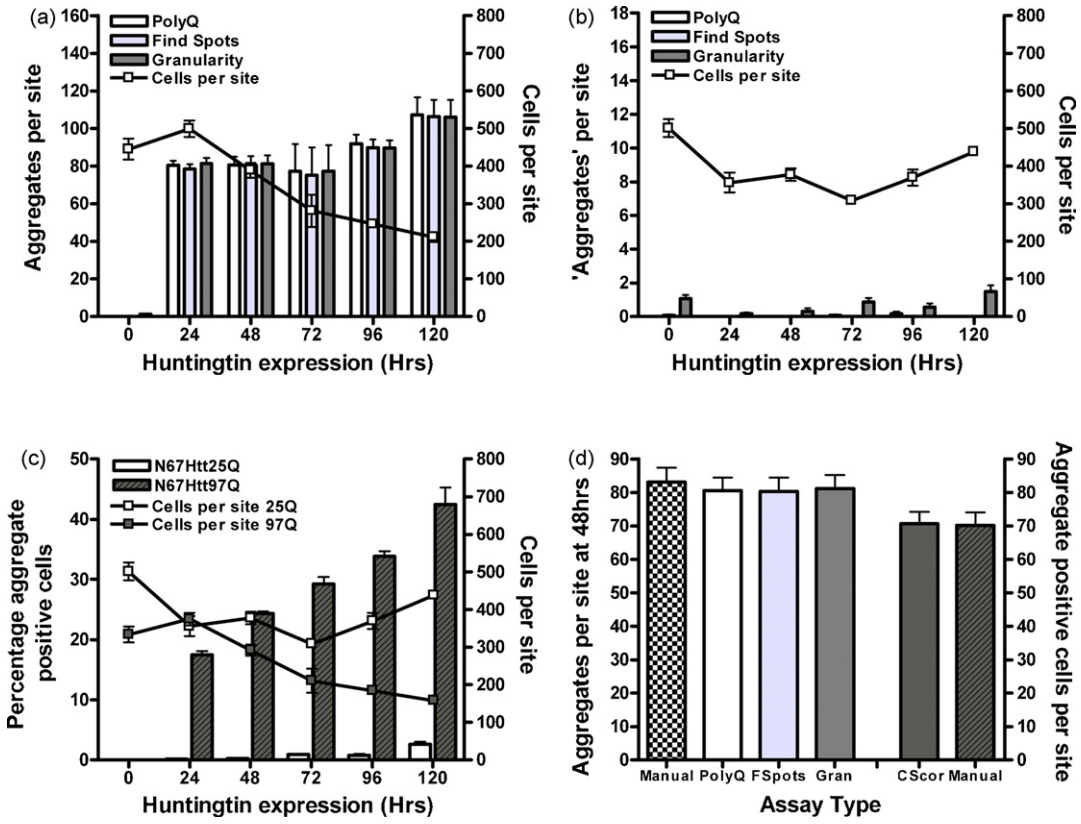

Fig. 3. (A) Number of cells (depicted by the squares joined by the line) and number of aggregates (bars) counted per image (site) in PC12 N67Htt97Q cells induced to express mutant huntingtin for various durations using three of the analysis assays. (B) Number of cells (depicted by the squares joined by the line) and number of false positives aggregates (bars) counted per image (site) in PC12 N67Htt25Q cells induced to express normal huntingtin for various durations using three of the analysis assays. (C) Number of cells (depicted by the squares joined by the line) and percentage of aggregate positive cells (bars) counted per image (site) in PC12 N67Htt25Q or N67Htt97Q cells induced to express normal or mutant huntingtin for various durations using the Cell Scoring assay. (D) Accuracy of the four analysis methods. Automated counts of aggregates per site at 48 h are not significantly different from manual counting ($F = 1.486$, not significant). Newman–Keuls Multiple Comparison Tests also showed that there were no significant differences between any of the analysis methods. The Cell Scoring assay correlates more closely with a second manual count of the number of positive cells per site rather than the aggregates per site count.

Comparing the image analysis results with the results obtained by manual cell counting at 48 h showed that all automated assays correlated significantly with the manual count data: PolyQ Pearson's $r = 0.9663$ ($P < 0.0001$); Find Spots Pearson's $r = 0.9722$ ($P < 0.0001$); Granularity Pearson's $r = 0.9792$ ($P < 0.0001$), Cell Scoring Pearson's $r = 0.9590$ ($P < 0.0001$). To determine the accuracy of the aggregate counting we performed a one-way ANOVA with Newman–Keuls Multiple Comparison Tests comparing the absolute numbers of aggregates counted per image using the manual and automated image analysis methods. None of the assays, including Cell Scoring, produced a significantly different count to the manual count ($F = 1.486$, not significant), indicating that they are each able to count absolute numbers of aggregates in excellent agreement with one another and the manual counts (Fig. 3D).

However, as depicted in Fig. 3D, the Cell Scoring assay had a tendency to count fewer aggregates per site. The Cell Scoring assay measures the proportion of cells possessing aggregates by including only those aggregates which are associated with a cell and only the first aggregate in any cell as a positive 'hit'. The disparity in aggregate counts between Cell Scoring and the other three assays thus arises from the exclusion of counts from both extracellular aggregates (Fig. 4, closed arrow) and multiple aggregates per cell (Fig. 4, open arrows). For this reason a second manual count was performed on merged images of aggregates and nuclei, this time counting cells as 'positive' (containing an aggregate) or 'negative' (not containing an aggregate) in order to assess the true accuracy of Cell Scoring. This manual counting took approximately 2 min 55 s per image while the automated Cell Scoring assay required only 19.5 s per image. A paired t-test showed no significant difference between this second manual count and the automated assay ($t = 0.3025$, d.f. = 15, ns) indicating that it accurately counted aggregates in cells and excluded aggregates not associated with cells. For cell lines such as PC12s, which are susceptible to the cytotoxic effects of mutant huntingtin expression and therefore leave non cell-associated aggregates, measuring the percentage of cells with aggregates rather than simply normalising aggregates to cell number gives a more accurate representation of the data.

By applying all analyses to both PC12 N67Htt97Q cells, which form huntingtin-EGFP aggregates, and PC12 N67Htt25Q cells, which do not, we have also been able to assess the frequency of 'false positives' counted by each analysis tool. Fig. 3 shows that the Cell Scoring assay (Fig. 3C) and to a lesser extent the Granularity assay detected false positives but the PolyQ and Find Spots assays did not (Fig. 3B). Furthermore, some of our assays can also determine aggregate size. For aggregate size determination we have found that the PolyQ assay works best (Fig. 5).

In combination with the Discovery-1^{TM} automated image acquisition platform, the Metamorph^{TM} assays described here each present powerful methods of quantifying protein aggregates in a range of disorders, although the assays vary in both their throughput and accuracy. Cell Scoring, which assesses only the proportion of positive cells (the proportion of Hoechst-positive nuclei which have aggregates within the specified distance from the nucleus margin) presents an excellent method for quantifying aggregate formation without bias from cell death. Where cell death is negligible, the PolyQ, Find Spots and Granularity assays can all rapidly

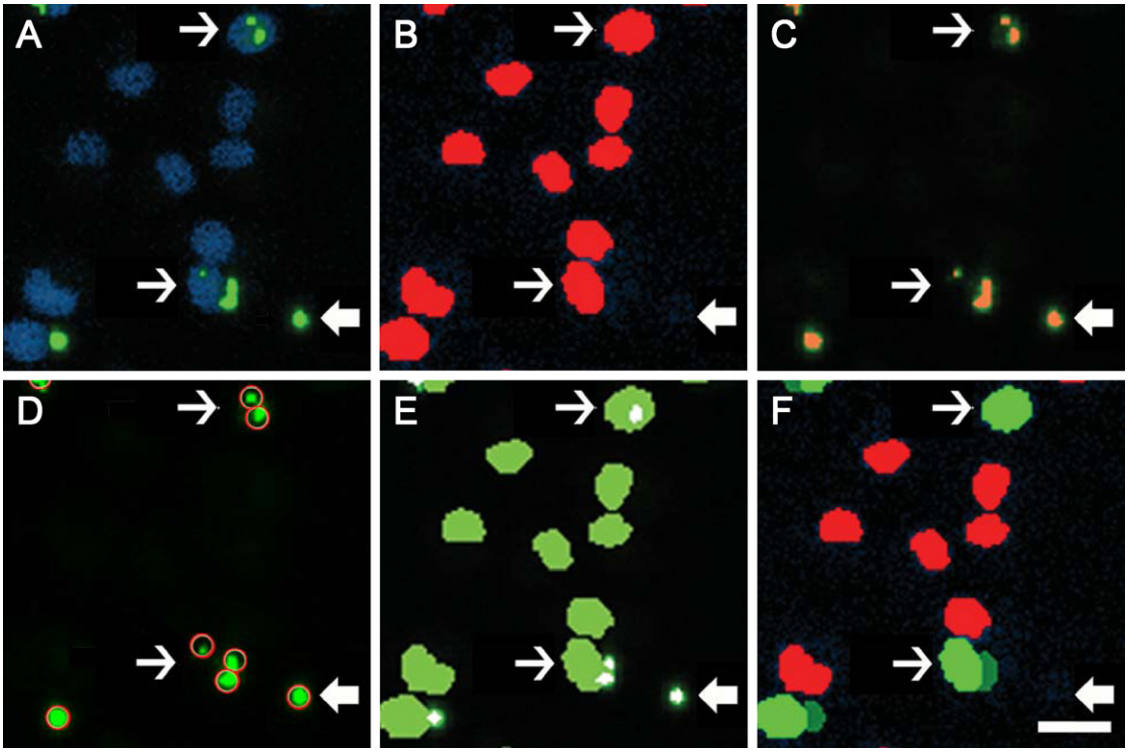

Fig. 4. Photomicrograph of the four analysis methods: (A) original image of Hoechst-stained cell nuclei with huntingtin-EGFP depicting instances of multiple aggregates per cell (open arrows) and aggregates with no associated nucleus (closed arrow). (B) Count nuclei analysis: all positive nuclei that meet the width and intensity criteria specified by the user shown in red. (C) PolyQ algorithm: all objects with staining intensity above a specified gray-level are digitally thresholded (orange overlay) and total area is measured. All thresholded objects are divided by an average aggregate size to generate a total aggregate count. (D) Find Spots algorithm: objects meeting user defined size and intensity parameters are identified and counted (red circles). (E) Granularity algorithm: counted granules (aggregates) meeting user defined parameters shown white and counted nuclei green. (F) Cell scoring assay with counted nuclei and their associated objects shown green and dark green, respectively. Aggregate-negative nuclei are shown red. Scale bar = 50 μm. (For interpretation of the references to color in this figure legend, the reader is referred to the web version of the article.)

and accurately quantify the number of aggregates of mutant protein per analysis site, with our in-house PolyQ assay providing the fastest analysis. Although we applied these assays to quantify aggregates in cell culture they can also be applied to determine, at high throughput, aggregates in images acquired from tissue sections. Furthermore, images acquired on other microscope platforms can also be analyzed at high throughput using these Metamorph™ (and other similar) analysis tools.

The high throughput image analysis tools described here allow rapid analysis of cell death and aggregate formation, providing a powerful platform for the screening of novel compounds and other therapeutic approaches. As HD is just one of many diseases which are characterised by mutant protein aggregation these high throughput image-based methods are likely to be applicable to a range of disorders, and therefore be of considerable interest to researchers and the pharmaceutical industry.

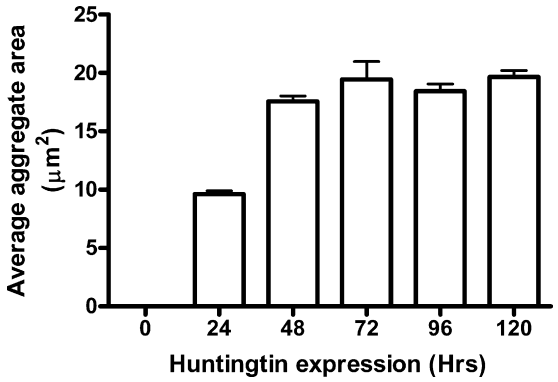

Fig. 5. Graph showing average aggregate area (μm²) determined using the PolyQ assay plotted against time. Aggregate size increases over time as determined by a one-way ANOVA ($F = 158.3$, $P < 0.0001$). Post hoc Newman–Keuls Multiple Comparison Tests showed significant increases in the average aggregate area starting at 24 h increasing again significantly at 48 h and then plateauing.

Acknowledgements

This work was supported by grants from the Marsden Fund of New Zealand, the Health Research Council and the National Research Centre for Growth and Development. ELS was supported by the Neurological Foundation of New Zealand and The University of Auckland, PN was supported by the National Research Centre for Growth and Development. The cell line used in this paper was kindly gifted by Dr. Eric Schweitzer (Brain Research Institute, UCLA). Dow Agrosciences kindly provided the insect steroid hormone tebufenozide for induction of the cell lines.

References

Aiken CT, Tobin AJ, Schweitzer ES. A cell-based screen for drugs to treat Huntington's disease. Neurobiol Dis 2004;16:546–55.
Arrasate M, Mitra S, Schweitzer ES, Segal MR, Finkbeiner S. Inclusion body formation reduces levels of mutant huntingtin and the risk of neuronal death. Nature 2004;431:805–10.
Berthelier V, Wetzel R. Screening for modulators of aggregation with a microplate elongation assay. Methods Enzymol 2006;413:313–25.
Chen S, Berthelier V, Yang W, Wetzel R. Polyglutamine aggregation behavior in vitro supports a recruitment mechanism of cytotoxicity. J Mol Biol 2001;311:173–82.
Corcoran LJ, Mitchison TJ, Liu Q. A novel action of histone deacetylase inhibitors in a protein aggresome disease model. Curr Biol 2004;14:488–92.
Hamuro L, Zhang G, Tucker TJ, Self C, Strittmatter WJ, Burke JR. Optimization of a polyglutamine aggregation inhibitor peptide (QBP1) using a thioflavin T fluorescence assay. Assay Drug Dev Technol 2007;5:629–36.

Heiser V, Engemann S, Brocker W, Dunkel I, Boeddrich A, Waelter S, et al. Identification of benzothiazoles as potential polyglutamine aggregation inhibitors of Huntington's disease by using an automated filter retardation assay. Proc Natl Acad Sci 2002;99:16400–6.

Kato M, Kinoshita H, Enokita M, Hori Y, Hashimoto T, Iwatsubo T, et al. Analytical method for B-amyloid fibrils using CE-laser induced fluorescence and its application to screening for inhibitors of B-amyloid protein aggregation. Anal Chem 2007;79:4887–91.

Kazantsev A, Preisinger E, Dranovsky A, Goldgaber D, Housman D. Insoluble detergent-resistant aggregates form between pathological and nonpathological lengths of polyglutamine in mammalian cells. Proc Natl Acad Sci 1999;96:11404–9.

Kitamura A, Kubota H, Pack CG, Matsumoto G, Hirayama S, Takahashi Y, et al. Cytosolic chaperonin prevents polyglutamine toxicity with altering the aggregation state. Nat Cell Biol 2006;8:1163–70.

Muchowski PJ, Schaffar G, Sittler A, Wanker EE, Hayer-Hartl MK, Hartl FU. Hsp70 and hsp40 chaperones can inhibit self-assembly of polyglutamine proteins into amyloid-like fibrils. Proc Natl Acad Sci 2000;97:7841–6.

Ravikumar B, Vacher C, Berger Z, Davies JE, Luo S, Oroz LG, et al. Inhibition of mTOR induces autophagy and reduces toxicity of polyglutamine expansions in fly and mouse models of Huntington disease. Nat Genet 2004;36:585–95.

Sanchez I, Mahlke C, Yuan J. Pivotal role of oligomerization in expanded polyglutamine neurodegenerative disorders. Nature 2003;421:373–9.

Saudou F, Finkbeiner S, Devys D, Greenberg ME. Huntingtin acts in the nucleus to induce apoptosis but death does not correlate with the formation of intranuclear inclusions. Cell 1998;95:55–66.

Scherzinger E, Sittler A, Schweiger K, Heiser V, Lurz R, Hasenbank R, et al. Self-assembly of polyglutamine-containing huntingtin fragments into amyloid-like fibrils: implications for Huntington's disease pathology. Proc Natl Acad Sci USA 1999;96:4604–9.

Skogen M, Roth J, Yerkes S, Parekh-Olmedo H, Kmiec E. Short G-rich oligonucleotides as a potential therapeutic for Huntington's disease. BMC Neurosci 2006;7:65.

Suhr ST, Gil EB, Senut MC, Gage FH. High level transactivation by a modified Bombyx ecdysone receptor in mammalian cells without exogenous retinoid X receptor. Proc Natl Acad Sci 1998;95:7999–8004.

The Huntington's Disease Collaborative Research Group. A novel gene containing a trinucleotide repeat that is expanded and unstable on Huntington's disease chromosomes. Cell 1993;72:971–83.